

Transmission electron microscope study of imperfections in type I diamond

P. P. PHAKEY AND P. R. W. HUDSON

Department of Physics, Monash University, Clayton, Victoria 3168, Australia

Transmission electron microscope (TEM) study of a normal I_a diamond showed that giant platelets and intermediate platelets were present on {100}. The crystallographic shape of the intermediate platelets and the presence of dislocations bounding them makes them different from the ordinary small platelets commonly observed in I_a diamond. TEM study of a natural I_b diamond revealed the presence of small nearly spherical defects which may be voids, bubbles of hydrogen, amorphous material or crystalline material of a low structure factor. Some of these small defects look like minute platelets.

1 INTRODUCTION

Type I diamonds are usually divided into two categories depending upon the concentration and the nature of the nitrogen impurity. The nitrogen concentration in type I_a is high (~ 500) and is present in a non-paramagnetic form. In type I_b diamond the nitrogen concentration is low (~ 50 ppm). ESR studies show that some of the nitrogen in I diamond is present in substitutional sites (Smith *et al* 1959).

Platelets on {100} responsible for anomalous X-ray spots are a characteristic feature of I_a diamond (Lonsdale 1942, Takagi & Lang 1964). These platelets are believed to be extrinsic faults which extend the diamond lattice by $1/3a_0$ in a direction perpendicular to the platelets; a_0 being the unit cell length (Hoerni & Wooster 1955). Elliot (1960) suggested that platelets are aggregates of nitrogen atoms while Lang (1964) proposed the most satisfactory model for the nitrogen in the platelets. There is a correlation between the infra-red absorption at $7.3 \mu\text{m}$ and the integrated spike intensity (Sobolev *et al* 1968, Evans & Ramey 1975). Recently arguments have been presented to emphasize that nitrogen is not the major constituent of the platelets (Davies 1970, Berman *et al* 1975, Evans & Ramey 1975, Evans 1976).

The first direct observation of platelets in type I_a diamond using transmission electron microscopy was made by Evans & Phaal (1962) and then by James & Evans (1965). These platelets were found to have a linear dimension between 100 \AA and 1000 \AA . Much larger ($\approx 80 \mu\text{m}$) platelets or planar defects also lying on {100} were observed by cathodoluminescence (Mendelssohn 1971) and by X-ray topography (Hanley *et al* 1976). Direct observation by TEM

of giant platelets in an unusual natural gem diamond has been reported by Hudson & Phakey (1976). Woods (1976) has also made similar observations. Possible platelet structures have been the subject of much discussion (Evans & Rainey 1975, Evans 1976, Hudson 1976). This paper reports a transmission electron microscope study of a I_a diamond which contained giant and intermediate platelets, and a I_b diamond which showed a type of defect not previously reported in diamond.

2 EXPERIMENTAL

The specimens for investigation were obtained from the Diamond Research Laboratory, Johannesburg and were in the form of cubes of side 2 mm. The specimens were examined with a polarizing microscope to determine their birefringence structure. From the observed birefringence and ultraviolet and infrared absorption measurements, two specimens were selected. The first specimen was a moderate I_a diamond; its birefringence was high but the birefringence patterns were anisotropic with respect to the three cube directions. The I_b sample had an amber colour and extremely low birefringence. Electron spin resonance of this specimen confirmed it was a I_b sample.

For transmission electron microscopy a thin slice (thickness 0.5 μm) was cut parallel to (100) from each of the selected specimens. These slices were mechanically ground and polished on both sides until they were about 100 μm thick. A nickel slotted grid was then glued on to the slice to strengthen it for handling. The grid mounted diamond slice was thinned by argon beam bombardment (nominally 5 kV potential) until a small perforation appeared in the sample. The areas near the edges of the perforation were suitable for electron transmission. This method has advantages over the oxidation technique (Evans & Phaal 1962, James & Evans 1965) which produces random fragments of the sample. Ion beam thinning allows a study to be made of selected areas in the sample. Retinning of the foil to enlarge the perforation and expose new areas can be done readily. Moreover the foil is strong enough to carry out further examination by other techniques.

3. OBSERVATIONS AND RESULTS

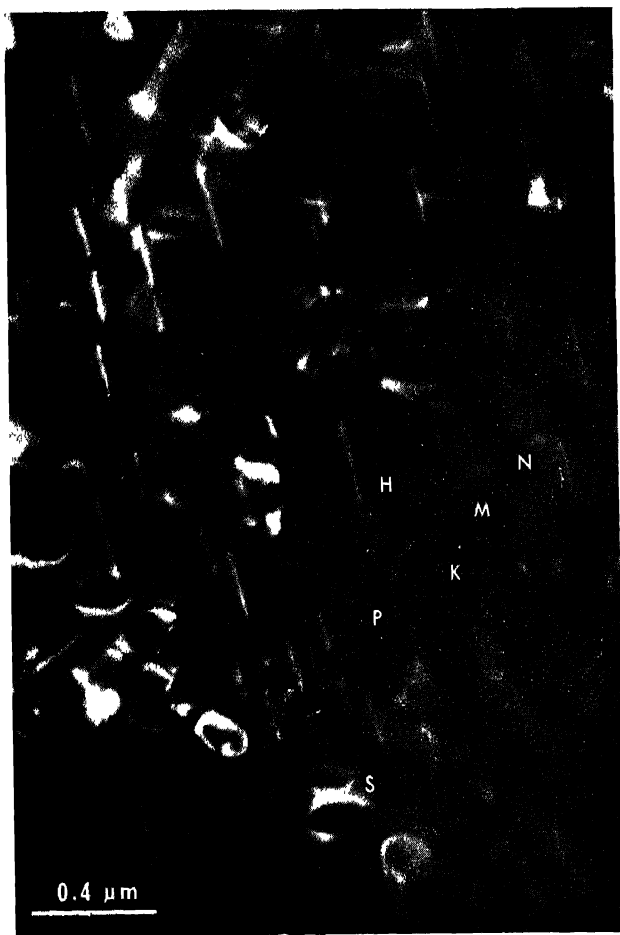
3.1. Type I_a Diamond

TEM observations of our sample showed that it was inhomogeneous as it contained three types of regions each with its own characteristic microstructure. Intermediate size platelets lying in {100} with their longest side ranging from 1000 to 3000 Å were found to be concentrated mainly in two bands of approximate width 5 μm and 16 μm respectively. The boundaries between the platelet-rich bands and the adjoining material were well defined (parallel to $\langle 110 \rangle$);



Fig. 1. Dark field (DF) micrographs showing a portion of a band rich in intermediate platelets. Figures 1a and 1b are of nearly the same area.

(a) Electron beam along $[001]$. Edge on dislocation in (100) and (010) show an oscillatory contrast similar to inclined dislocations. Some of these are labelled to enable a comparison with (b). Platelets in (001) are hard to see.



(b) Specimen is tilted from (a) (100) platelets are inclined and show dislocations bounding them (Discussed in the text); Compare labelled features in (a) and (b) Platelets in (001) are also visible. Notice the geometrical shape of the platelets



Fig. 2 Bright field (BF) micrograph showing the boundary between a band rich in intermediate platelets and the adjoining material. Platelets in (100) and (010) are nearly edge on and show an oscillatory contrast similar to inclined dislocations. The weak image labelled C shows the outline of a platelet in (001).



Fig. 3 BF micrograph showing dislocations. *P* labels inclined platelets showing fringes. Notice dislocation *D* (discussed in text) at a platelet.



Fig. 4 A typical example of giant platelets *A* and *B* on (100) and (010) respectively. Notice dislocations *D* in *A* and dislocations *B'* at the end of the platelets. BF micrograph.



Fig. 5a. BF micrograph of small (common) platelets in I_n diamond. Notice extensive strain field around the platelets



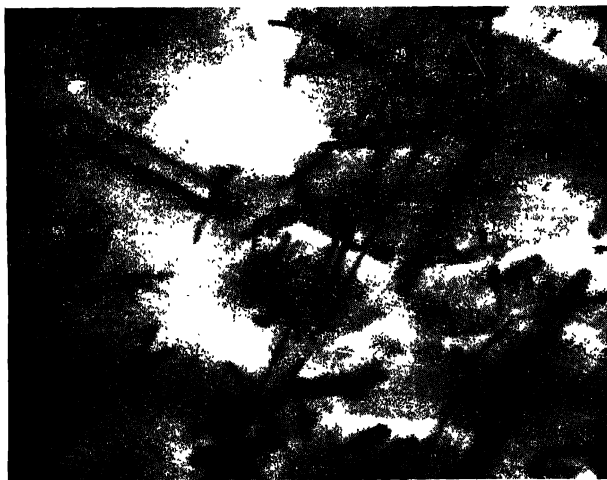
5b DF micrograph Small platelets are inclined and show fringes



Fig. 6 BF micrograph. Intermediate platelets are melted to the electron beam direction. Platelets in (100) and (010) show fringes. Some of the platelets in (001) are labelled C. Notice that the platelets are bounded by well defined sides parallel to ± 011 .



Fig 7 BF micrographs. Intermediate platelets are inclined to the electron beam direction.
(a) Platelets, some of which are labelled, show fringes and bounding dislocations.



(b) Nearly the same area as in (a). Fringes at the platelets are out of contrast. Comparison with the features labelled in (a) shows the dislocations bounding the platelets.



Fig. 8 Small defects in a I_b diamond showing structure factor contrast. Edge of the specimen is labelled E. BF micrograph.

for examples see figures 1 and 2. In the second region dislocations predominated but some intermediate size platelets were also present (figure 3). The bulk of the specimen formed the third type of region in which giant platelets (also in $\{100\}$) of length $1\text{ }\mu\text{m}$ to greater than $5\text{ }\mu\text{m}$ were present (figure 4). Both intermediate and giant platelets differed from the normal type of small platelets (diameter 200 to 1000 Å) commonly found in I_a diamond. In figure 5 an example of these small (common) platelets is shown for the purpose of comparison with the ones found in our sample. When viewed edge on, or nearly so, these small platelets formed sharp images and showed a considerable strain field around them (figure 5a). When inclined to the electron beam direction, fringes were seen to mark the platelets (figure 5b) but there was no evidence to indicate that these platelets were bounded by dislocations; this point will be discussed later.

TEM observation of giant platelets have been reported by Hudson & Phakey (1976). It was found that when these platelets were seen edge on, they formed sharp images showing negligible strain. When they were inclined to the electron beam direction, diffraction contrast fringes were observed. From the study of the fringe pattern a fault vector of approximately $1/4\langle 101 \rangle$ was found to be associated with them (Hudson & Phakey 1976). The platelets were found to terminate at dislocations although some dislocations could also be seen along the longer platelets (figure 4).

When the intermediate platelets in our sample were viewed edge on their images always showed an oscillatory contrast (see figures 1a and 2). On slightly tilting the platelets from the edge on orientation, the oscillatory contrast still persisted. Larger tilts showed diffraction contrast fringes at the $\{101\}$ and $\{100\}$ platelets (figure 6). The outline of the fringes revealed that these platelets were bounded by well defined sides parallel to $\langle 101 \rangle$ which gave the $\{010\}$ and $\{100\}$ platelets a *diamond* shaped appearance, whereas the $\{001\}$ platelets had a square or a rectangular look (figure 6). In general the $\{001\}$ platelets were hard to see in micrographs when they lay normal to the electron beam direction; for example see the platelet labelled *C* in figure 2. Another important observation made from larger tilts of the specimen was that these platelets were bounded by dislocations, for example see figures 3 and 7. Although the presence of fringes has complicated the contrast from dislocations in figures 7a, a comparison with figure 7b readily identifies them. A better example is shown in figure 1b where the dislocations bounding the platelets can be seen very clearly. The set of platelets revealing these dislocations is edge on in figure 1a as can be seen from the comparison of features labelled in both figures 1a and 1b. It should be noted that such dislocations were not seen to be associated with the small (common) platelets. It is therefore, quite clear that the oscillatory contrast shown

by the intermediate platelets is mainly due to the dislocations bounding them.

Sufficient diffraction contrast information is not yet available for the fringe patterns observed at the intermediate platelets. It is, therefore, not possible to find a unique fault vector for them. From X-ray data the fault vector for the small (common) platelets is expected to be $1/3 \langle 100 \rangle$ (Hoerni & Wooster 1955) whereas TEM studies (Hudson & Phakey 1976) suggest that the fault vector for small (common) platelets is expected to be $1/3 \langle 100 \rangle$ (Hoerni & Wooster 1955) whereas TEM studies (Hudson & Phakey 1976) suggest that the fault vector for the giant platelets is probably $\approx 1/4 \langle 101 \rangle$ although Woods (1976) favours

$1/3 \langle 100 \rangle$. However, from limited diffraction contrast information obtained by us on intermediate platelets it was not possible to distinguish between $1/3 \langle 100 \rangle$ and $1/4 \langle 101 \rangle$.

3.2 *Type I_b Diamond*

The specimen thinned at a very fast rate $\approx 3 \mu\text{m/hr}$. cursory TEM examination seemed to indicate that the specimen was free from defects because the known defects in diamond such as platelets (small, intermediate or giant) or dislocations were not seen. However, when the tilt of the specimen was adjusted to give sharp thickness fringes near the edge of the perforation in the specimen, small defects showing black and white dots were seen near the edges of the thickness contours or fringes. An example of this is shown in figure 8 where white dots are seen on the thin side of the black thickness fringe (that is, towards the edge of the specimen), black dots are seen on the thin side of the adjacent light thickness fringes, and no dots are seen near the centre of the fringes. Also notice in figure 8 that the images (dots are most pronounced in the thin areas of the foil). When they occur in thicker parts of the foil the effective contrast is reduced because of increased absorption in the crystal.

The observations described here fit the description of the common type of structure factor contrast usually observed when a small inclusion (precipitate, void etc.) has a structure factor different from the matrix, and hence a different extinction distance (Ashby & Brown 1963). It has been shown (Ashby & Brown 1963) that an inclusion of thickness ΔZ would change the effective foil thickness, Z , in columns of crystal containing the inclusion by an amount (at $s = 0$) given by

$$t_0 \Delta Z \left(\frac{1}{t_{0p}} - \frac{1}{t_0} \right)$$

where t_{0p} and t_0 are the relevant extinction distances in the inclusion and the matrix respectively. The nature of the contrast shown by the inclusion depends

upon whether t_g^p is greater than or less than t_g as is shown in figure 9. It can be seen that our observations are identical with those predicted in figure 9c where $t_g < t_g^p$. Obviously this type of contrast would be shown by voids (holes) or amorphous regions because for them $t_g^p = \infty$.

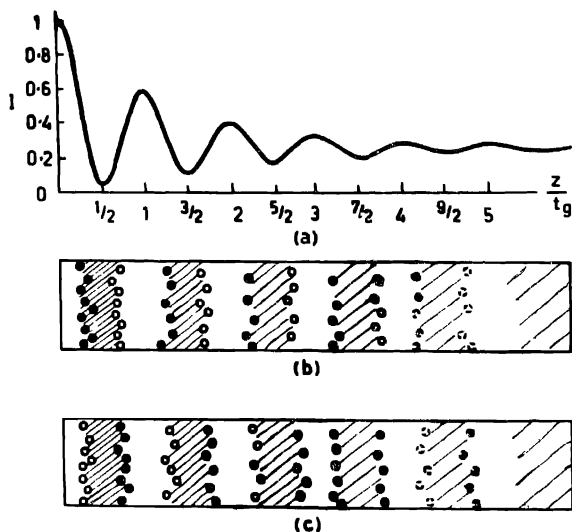


Fig. 9 Correlation between intensity oscillations (thickness fringes) and the position of dark and bright images for small inclusions. After Ashby and Brown (1963).

- (a) Intensity oscillations with increasing thickness
- (b) Position of images when $t_g > t_g^p$.
- (c) Position of images when $t_g < t_g^p$.

Critical examination of these defects using an electron microscope which was capable of very high point to point resolution showed that some of the defects were not exactly spherical in shape but they were slightly elongated. Using the *weak beam* technique (Cockayne, Ray & Whelan 1969) for image formation it was confirmed that a good many of them were elongated and looked like minute platelets on (100).

4. DISCUSSION

There seems to be a basic difference between the intermediate platelets (longest dimension 1000 to 3000 Å) found in our sample and the more common small platelets (diameter 100 to 1000 Å) found generally in I_a diamond. The

small platelets form sharp images, have an intensive strain field normal to them, and are not bounded by dislocations. On the other hand the intermediate platelets have negligible strain, have a geometrical shape, and are bounded by dislocations. These differences can be explained on a simplified model described below.

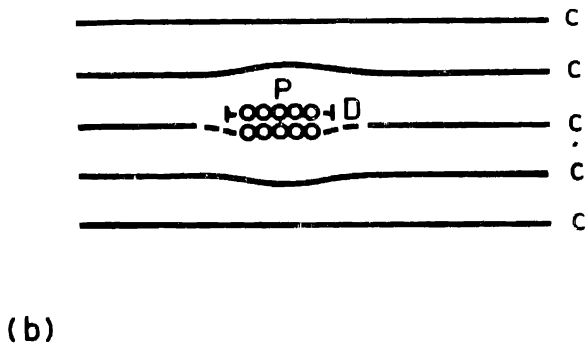
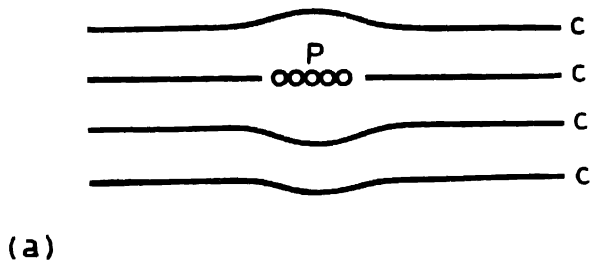


Fig. 10. Simplified model for platelets in I_a diamond

- (a) Small (normal) platelet, P . No dislocation is present at the periphery of the platelet.
- (b) Intermediate platelet, P . Dislocation D bounds the periphery of the platelet.

A simplified model for the small platelets can be given. According to this model small platelet is a concentration of some kind of impurity atom which has been substituted for the regular C atoms in a localized area on a $\{100\}$ plane in diamond as shown in figure 10a. This type of platelet would possess a strain

field normal to it depending upon the difference between the size of the impurity atom and the C atom, and it will have coherent interfaces. Since the impurity atoms forming the platelet are in substitutional sites in a plane which belongs to the diamond lattice, a dislocation is not introduced. If a platelet of this kind grows in thickness as shown in figure 10b, the increase in strain resulting from the mismatch can be alleviated if dislocations bound the periphery of the precipitate. (This case is similar to a prismatic loop surrounding an extrinsic stacking fault). Such a precipitate would still have coherent interfaces if no dislocations are present in its plane. The intermediate platelets in our sample may be of this kind. Naturally the energy associated with the platelet would be reduced if the platelet takes a crystallographic shape and the surrounding dislocations take a low energy configuration. This has been observed for the intermediate platelets described in section 3.1. It was suggested earlier (Hudson & Plakcy 1976) that this diamond has been subjected to higher temperatures and pressures at some stage in its natural history. Such treatment would favour growth of platelets and make attain a crystallographic shape. A further growth in size and thickness would result in a giant platelet which in certain circumstances may need more dislocations along its faces to alleviate extensive strains; the interfaces will thus be partly coherent.

Observations indicate that the small defects observed in our I_b diamond sample have an extinction distance greater than that of the surrounding matrix. That is the structure factor, F , of the small defects is less than the matrix which is diamond. It is not possible to determine the exact nature of these defects but voids, bubbles of gas and/or liquid, amorphous material or crystalline material of a low structure factor are all consistent with the results. There is some evidence that hydrogen is present in diamond (Kaiser & Bond 1959, Melton & Giardini 1974, 1975, 1976) and in particular, in this specimen (Hudson & Tsong 1976), the hydrogen might be present in the bubbles. Since some of these small defects were found to be slightly elongated, they looked like minute platelets on {100}. It is possible that these are minute platelets and are not different (except in size) from the common variety of small platelets found in I_a diamond.

ACKNOWLEDGMENTS

We thank the Diamond Research Laboratory for the diamond samples.

REFERENCES

- Ashby M. F. & Brown I. M. 1963 *Phil. Mag.* **8**, 1649.
Borman R., Hudson P. R. W. & Martinez M. 1975 *J. Phys. C: Sol. St. Phys.* **8**, L430.
Cookayne D. J. H., Ray I. L. F. & Whelan M. J. 1969 *Phil. Mag.* **20**, 1265.
Davies G. 1970 *Nature, Lond.* **228**, 758.
Elliott R. J. 1960 *Proc. Phys. Soc. Lond.* **76**, 787.
Evans T. 1976 *Contemp. Phys.* **17**, 45.

- Evans T. & Phaal C. 1962 *Proc. R. Soc. Lond.* **A270**, 538.
 Evans T. & Rainey P. 1975 *Proc. R. Soc. Lond.* **A344**, 111.
 Hanley P., Kiflawi I. & Lang A. R. 1976 *Phil. Trans. Roy. Soc.* (In press).
 Hoerni J. A. & Wooster W. A. 1955 *Acta. Cryst.* **8**, 187.
 Hudson P. R. W. 1976 *Phys. Stat. Sol. (a)* (in press).
 Hudson P. R. W. & Phakey P. P. 1976 *Phys. Stat. Sol. (a)* **36**, 627.
 Hudson P. R. W. & Tsong I. S. T. 1976 *Proc. 2nd. Nat. Phys. Cong. Sydney* p. 128 (to be published).
 James P. F. & Evans T. 1965 *Phil. Mag.* **11**, 123.
 Kaiser W. & Bond W. L. 1959 *Phys. Rev.* **115**, 857.
 Lang A. R. 1964 *Proc. Phys. Soc. Lond.* **84**, 871.
 Lonsdale K. 1942 *Proc. R. Soc. Lond.* **A179**, 315.
 Molton C. E. & Giardini A. A. 1974 *Am. Miner.* **59**, 775.
 Molton C. E. & Giardini A. A. 1975 *Am. Miner.* **60**, 413.
 Molton C. E. & Giardini A. A. 1976 *Nature* **263**, 309.
 Mondelssohn M. J. 1971 *Ph.D. Thesis*. University of London.
 Smith W. V., Sorokin P. P., Gelles I. L. & Lasler G. J. 1959 *Phys. Rev.* **115**, 1546.
 Sobolev E. V., Lisovyan V. I. & Lenskaya S. V. 1968 *Sov. Phys. Dokl.* **12**, 665.
 Takagi M. & Lang A. R. 1964 *Proc. R. Soc. Lond.* **A281**, 310.
 Woods G. S. 1976 (to be published).